JOURNAL OF MATERIALS SCIENCE 32 (1997) 3219–3225

The magnetic properties of Fe-based amorphous ribbons coated with various oxides using the sol–gel process

S. H. LIM, T. H. NOH
Magnetic Materials Laboratory, Korea Institute of Science and Technology, P.O. Box 131, Cheongryang, Seoul, 130–650, Korea.

Y. J. BAE, H. K. CHAE
Department of Chemistry, Hankuk University of Foreign Studies, Seoul, 130–791, Korea

Y. S. CHOI
Department of Metallurgical Engineering, Korea University, Seoul, 136–701, Korea

The metal oxides MgO, BaO, Al_2O_3, SiO_2, MgO–Al_2O_3, CaO–Al_2O_3, SrO–Al_2O_3, BaO–Al_2O_3 and MgO–SiO_2 have been coated onto ribbons of the Fe-based amorphous alloy Metglas 2605S3A using a sol–gel process. The effects of the surface coating on the magnetic properties of the alloy are investigated. The d.c. hysteresis loop for ribbons coated with MgO and MgO–Al_2O_3 is more square shaped than that for the uncoated ribbon. For ribbons coated with BaO, SrO–Al_2O_3 and BaO–Al_2O_3 it is more inclined than for the uncoated ribbon. Significant differences in the frequency dependence of the effective permeability are observed that depend on the nature of the coated oxides. The core loss is also affected by the coating. These results may be explained in terms of a stress induced by the coating and the modification of the domain structure via elastic and/or magnetoelastic interactions. It is thought from the magnetoelastic interactions that the MgO and MgO–Al_2O_3 coatings induce tensile stresses whilst those of BaO, SrO–Al_2O_3 and BaO–Al_2O_3 induce compressive stresses.

1. Introduction

Coatings are frequently applied to the surfaces of sheets or ribbons of magnetic materials in order to improve their properties. One important use of coatings is the reduction of eddy currents when the coating provides insulation between layers in stacked or tape wound cores. The coating can be produced by simply dipping the ribbons into a mixture of a fine oxide powder in water or organic solvents [1]. Another important use for coatings is the modification of domain structure via stresses induced by the coating. An example of this type of coating is that which is applied to silicon steel sheets in order to refine its domain structure [2–5], since the coated layer/matrix interface is able to transfer induced stress at the coated layer to the matrix. This type of coating is generally produced by more sophisticated methods.

Coatings applied to amorphous magnetic ribbons have so far been produced in order to achieve the first goal, namely, a reduction in eddy currents. Recently, however, a magnesium oxide coating on a zero magnetostrictive Co-based amorphous ribbon, created using the sol–gel process, was observed to also affect the a.c. and d.c. magnetic properties in addition to the eddy current loss [6]. As well as the reduction in core loss, it was found that the a.c. effective permeability was improved over the frequency range of 1–1000 kHz and also the d.c. hysteresis loops were inclined by the surface coating. These results were thought to be a result of the tensile stress induced by the coating, which in turn modifies the domain structure. Since the ribbon used had a nearly zero magnetostriction, the stress effect was considered to be mainly elastic. It is expected that, if a coating could be produced on a ribbon with a large magnetostriction then the effects of the coating on the magnetic properties would be even more pronounced, since the properties would now be influenced by both magnetoelastic and elastic interactions. It is therefore of interest to investigate the effects of surface coating on the magnetic properties of an amorphous ribbon with a large magnetostriction.

In this work, we employ a previously developed [6] sol-gel process to coat various oxide layers onto ribbons of an Fe-based amorphous alloy with a large magnetostriction and investigate the effects of the coatings on the magnetic properties of the alloy.

2. Experimental procedure

The amorphous alloy used was Metglas 2605S3A ($Fe_{76.6}Cr_2B_{16}Si_5C_{0.5}$) with a magnetostriction of 20×10^{-6} which was supplied by AlliedSignal Corp., USA. The width and thickness of the ribbon were

0022–2461

TABLE I The type of oxides and their precursor solutions, together with the concentrations of the metal alkoxides and water in ethanol and the thickness of the coated oxide layers

Type of oxide layer	Precursor solution in 2-methoxyethanol	Concentration of metal alkoxide (M)	Concentration of H_2O in ethanol (M)	Thickness of coated layer (μm)
MgO	$Mg(OCH_2CH_2OCH_3)_2$	0.5	0.5	0.70
BaO	$Ba(OCH_2CH_2OCH_3)_2$	0.5	0.5	0.40
Al_2O_3	$Al(OCH_2CH_2OCH_3)_3$	0.5	no water	0.39
SiO_2	$Si(OCH_2CH_3)_4$	0.06	0.24	0.65
$MgO–Al_2O_3$	$MgAl_2(OCH_2CH_2OCH_3)_8$	0.5	no water	0.75
$CaO–Al_2O_3$	$CaAl_2(OCH_2CH_2OCH_3)_8$	0.5	no water	1.92
$SrO–Al_2O_3$	$SrAl_2(OCH_2CH_2OCH_3)_8$	0.5	no water	1.68
$BaO–Al_2O_3$	$BaAl_2(OCH_2CH_2OCH_3)_8$	0.5	no water	1.80
$MgO–SiO_2$	$MgSi(OCH_2CH_2OCH_3)_6$	0.5	no water	1.39

4.48 mm and 15.5 μm, respectively. A variety of metal oxides; MgO, BaO, Al_2O_3, SiO_2, $MgO–Al_2O_3$, $CaO–Al_2O_3$, $SrO–Al_2O_3$, $BaO–Al_2O_3$, and $MgO–SiO_2$ were coated onto the alloy ribbons using the sol–gel process. The synthesis of the metal alkoxide precursors and complexes is described in detail elsewhere [7]. In this publication we present only a brief discussion of the technique. The solution of magnesium methoxyethoxide $[Mg(OCH_2CH_2OCH_3)_2]$ for the MgO coating was prepared by the reaction of an excess (8 mol) of 2-methoxyethanol ($CH_3OCH_2CH_2OH$, Aldrich) with one mole of magnesium ethoxide $[Mg(OCH_2CH_3)_2$, Aldrich]. Similarly, the other precursor solutions for single cation oxides were prepared by the exchange reaction of metal alkoxides with excess 2-methoxyethanol (in the cases of BaO and Al_2O_3) or ethanol (in the case of SiO_2). For bimetallic precursors, a solution of one metal alkoxide was added equivalent to a solution of the other metal alkoxide and the mixed solutions were then refluxed. Hydrolysis was carried out by adding a solution of water and alcohol to the precursor. The concentrations of the metal alkoxide and water in the precursor solution, which are important parameters in determining the thickness of the coated layer, were adjusted to give reasonable thickness values. For example, the concentration of water in ethanol was 0.5 M for MgO and BaO, and 0.24 M for SiO_2, whereas the concentration of metal alkoxide was 0.5 M for MgO and BaO, and 0.06 M for SiO_2. It was not necessary to add water to the other coatings, because the viscosity of the precursor solutions were already satisfactory to produce a reasonable thickness. The concentrations of the metal alkoxides and water used in this work are summarized in Table I. After dipping the alloy ribbon into the precursor solution, the ribbon was dried at 200 °C. All the coating procedures were carried out in a dry nitrogen atmosphere. The thickness of a coated layer was measured using a digital micrometer. In order to increase the accuracy of the measurement, a stack consisting of about 10–20 ribbons was first measured and the thickness of each ribbon was then obtained by dividing the total stack thickness by the number of ribbons in the stack. The results for the thickness of the coated oxide layer are also given in Table I. The measured thickness ranges from 0.39–1.92 μm. It is worth noting that the thickness of single cation oxides is generally much smaller than that of the mixed cation oxides.

The ribbons were wound onto toroidal cores with an inner diameter of 19 mm. The cores were annealed at 435 °C for 2 h under an N_2 gas atmosphere and then air-cooled. The a.c. effective permeability (μ_e) was measured using an impedance analyser at an applied field of 0.795 Am^{-1} and over a wide frequency range of 0.1–1000 kHz. D.c. magnetic properties were measured with a hysteresis loop tracer. The core loss (W_L) was measured by using a B–H analyser (Iwatsu Co. Model No. SY-8216) at frequencies up to 200 kHz and flux densities of 0.1, 0.3, 0.5, 0.7 and 1.0 T.

3. Results and discussion

In Fig. 1(a and b) we present the results for μ_e as a function of frequency. The results obtained on ribbons coated with single cation metal oxides are shown in Fig. 1a, whilst those for ribbons coated with the double metal oxides are shown in Fig. 1b. The results obtained for an uncoated ribbon are also shown on both figures. It can be seen from Fig. 1(a and b) that significant differences are observed in the frequency dependencies of the permeability. The ribbon coated with $MgO–Al_2O_3$ exhibits a substantially higher value of the permeability than the uncoated ribbon over the whole frequency range with the difference being larger at lower frequencies. The values for the ribbons coated with MgO and Al_2O_3 are also slightly higher than for the uncoated ribbon. The rest of the coated ribbons exhibit smaller values of the permeability than the uncoated ribbon at nearly all the frequencies. In the case of ribbons coated with BaO, $BaO–Al_2O_3$ and $SrO–Al_2O_3$, a peculiar behaviour in the frequency dependence of the permeability is observed; the effective permeability is very low at low frequencies, remains nearly constant up to 100 kHz and then slowly decreases with a further increase in the frequency. It is worth noting that, at the very high frequency of 1 MHz, the permeability of the coated ribbons is always higher than that of the uncoated ribbon. Some values of the permeability between 50–100 kHz are observed to be irregular, particularly for the ribbons coated with MgO and $MgO–Al_2O_3$. This phenomenon is considered to be due to

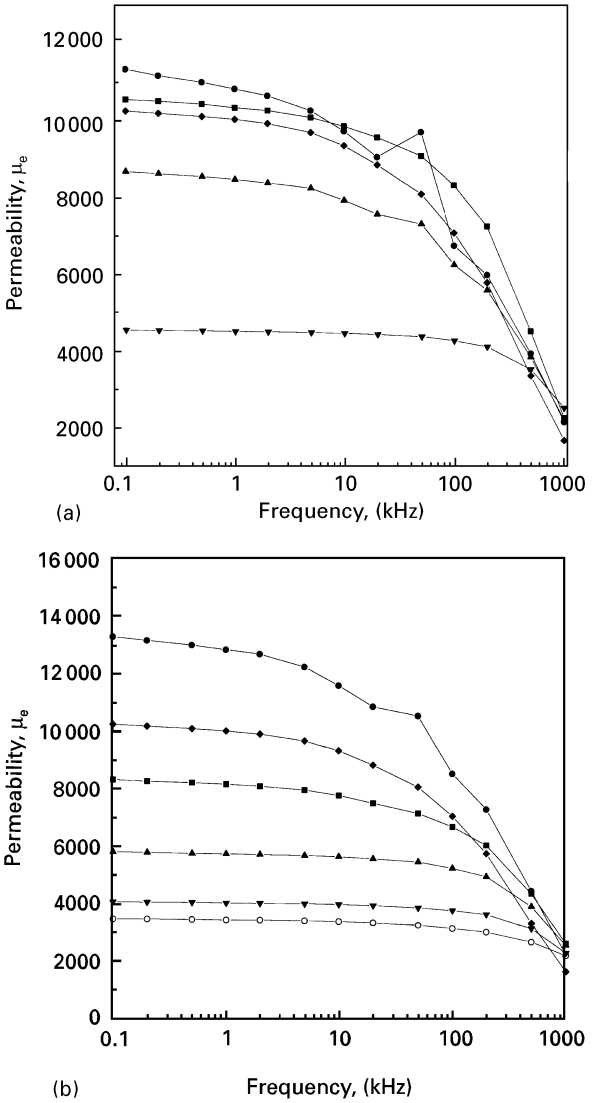

Figure 1 The value of effective permeability of Metglas 2605S3A as a function of frequency for the ribbons coated with (a) the single metal oxides (●) MgO, (■) Al_2O_3, (▲) SiO_2 and (▼) BaO and (b) the double metal oxides, (●) MgO–Al_2O_3, (■) MgO–SiO_2, (▲) CaO–Al_2O_3 (▼) BaO–Al_2O_3 and (○) SrO–Al_2O_3. The results for the uncoated ribbon are shown in both figures using the symbol (◆)

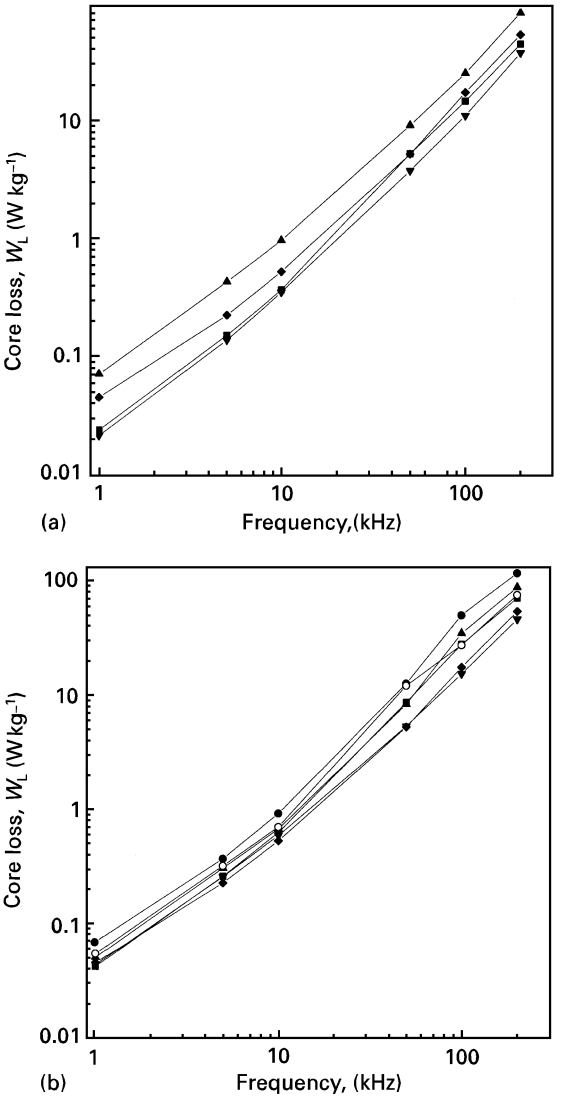

Figure 2 The value of core loss of Metglas 2605S3A at the flux density of 0.1 T as a function of frequency for the ribbons coated with (a) the single metal oxides; (■) Al_2O_3, (▲) SiO_2; (▼) BaO and (b) the double metal oxides; (●) MgO–Al_2O_3, (■) MgO–SiO_2, (▲) CaO–Al_2O_3 (▼) BaO–Al_2O_3 and (○) SrO–Al_2O_3. The results for the uncoated ribbon are shown in both figures using the symbol (◆) . Note: no core loss date for MgO coating at 0.1 T.

magnetomechanical resonance, which often occurs for highly magnetostrictive alloys [8].

The results for the core loss are shown in Figs 2(a and b) and 3(a and b) as a function of frequency at the fixed flux densities of 0.1 and 0.7 T, respectively. The results for the ribbons coated with a single oxide are shown in Figs 2a and 3a and those for the ribbons coated with the double metal oxides are shown in Figs 2b and 3b. The values of W_L were measured at various flux densities ranging between 0.1 to 1.0 T and the way in which W_L varies with frequency at the flux densities, not shown in this paper due to space limitations, is *qualitatively* similar to that shown in Figs 2(a and b) and 3(a and b) for the flux densities of 0.1 and 0.7 T. In the case of the ribbons coated with a single metal oxide, the difference in W_L is rather large depending on the oxides used in the coating. The core loss is higher than the uncoated ribbon for the ribbons coated with MgO and SiO_2 but is lower than the uncoated ribbon for those coated with Al_2O_3 and BaO. The same behaviour is observed at the other measured flux densities. In the case of ribbons coated with double metal oxides (Figs 2b and 3b), the frequency dependence of the core loss is somewhat different from that observed in Figs 2a and 3a in the case of ribbons coated with a single metal oxide. The difference between the W_L values is small and depends on the individual coating oxide. In addition the relative magnitude of W_L of the coated ribbons compared to the uncoated one changes with the flux density. At a flux density of 0.1 T, the uncoated ribbon has the lowest value of W_L at nearly all of the investigated frequency range. However, the relative magnitude of W_L of the uncoated ribbon progressively increases with the flux density and, at flux densities of 0.7 T and higher, the uncoated ribbon exhibits the largest value of W_L at nearly all the measured frequencies. This indicates that the importance of having a surface coating increases with the flux density. The same behaviour, namely a steady increase in the

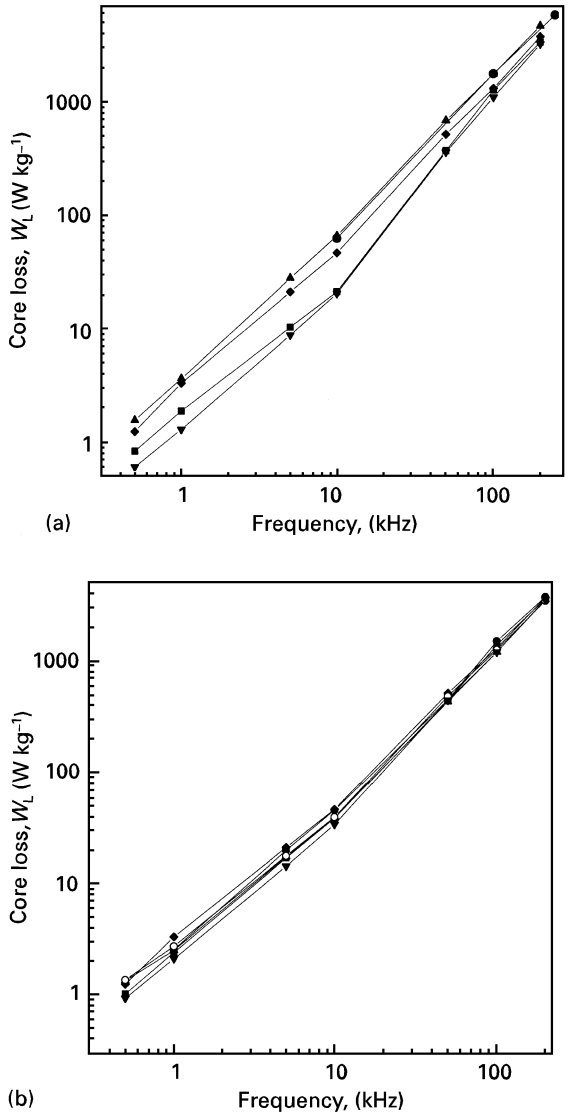

Figure 3 The value of core loss of Metglas 2605S3A at the flux density of 0.7 T as function of frequency for the ribbons coated with (a) the single metal oxides; (●) MgO, (■) Al_2O_3, (▲) SiO_2 and (▼) BaO and (b) the double metal oxides, (●) MgO–Al_2O_3, (■) MgO–SiO_2, (▲) CaO–Al_2O_3 (▼) BaO–Al_2O_3 and (○) SrO–Al_2O_3. The results for the uncoated ribbon are shown in both figures using the symbol (◆).

relative magnitude of W_L with the flux density, is also expected to occur for the ribbons coated with a single metal oxide. Actually, a closer examination of the core loss dependence on the frequency results for the ribbons coated with a single metal oxide does show the same behaviour. For example, the difference in W_L values between the SiO_2 coated and uncoated ribbons tends to decrease with the flux density, but, the gap between the BaO coated and uncoated ribbons increases with the flux density. This indicates that as the flux density increases the core loss characteristics of the coated ribbons improve to a greater extent than that of the uncoated ribbon. However, the change in the relative values between the coated and uncoated ribbons with the flux density does not occur in the case of ribbons coated with a single metal oxide. One reason for this may be that the difference in W_L values is large in this case. Amongst the ribbons coated with double metal oxides, the BaO–Al_2O_3 coated ribbon exhibits the lowest value of W_L at nearly all the measured frequencies and flux densities.

From the present results for μ_e and W_L, it is clear that there is no obvious correlation between the two properties, indicating that the major factors affecting the two individual properties differ from each other. The present results can be compared with those observed for a Co-based amorphous alloy, where both μ_e and W_L were improved by an MgO coating [6]. Although μ_e is often referred to as being the single most important property of a soft magnetic material, it is a highly complex function of both material parameters and microstructure. This quantity, μ_e, is closely related to the magnetization behaviour. The magnetization is created by domain wall movement and spin rotation, the relative contribution of each being a function of the frequency and the angle between the applied field and spin directions. The contribution to the magnetization by the spin rotation is known to be large when the frequency is high and the applied field direction is perpendicular to the spin direction [9, 10]. The magnetization mode of domain wall movement is significantly affected by the domain wall energy. The magnetization will be mainly created by the motion of a domain wall when the wall energy is large [11–13]. In this case the potential well produced by obstacles impeding the wall motion is an important factor. The obstacles include defects and internal (residual) stress, the latter being important for a material with a large magnetostriction such as the Metglas 2605S3A used in this work. The magnetization will be largely generated by wall bending if the wall energy is small and in this case the domain structure (refinement) is an important factor [11–13]. Magnetization by wall bending may be operating in the present amorphous alloy, since the wall energy is considered to be small due to a small anisotropy. The present results for μ_e may therefore be explained by considering the variation of domain structure with surface coating when the magnetization is mainly created by domain wall movement, namely the frequency is low and the proportion of the domains that are aligned in the length direction is high. The loss of cores subjected to an a.c. magnetic field may consist of a hysteresis loss and an eddy current loss. The core loss due to eddy currents may be further divided into classical eddy current loss and an anomalous loss [14, 15]. The classical eddy current loss is due to macroscopic eddy currents induced from homogeneous magnetization and it is independent of domain structure. On the other hand, the anomalous loss is due to microscopic eddy currents, which are induced from the dynamic movement of domain walls and are proportional to the wall velocity. Since amorphous alloy ribbons have a high resistivity and the thickness is very small, the classical eddy current loss is much smaller than the anomalous loss [15–18]. The total loss of amorphous alloy ribbons may therefore be understood by considering hysteresis loss and the anomalous loss. The hysteresis loss and the anomalous loss are proportional to the frequency and the frequency squared, respectively, so that the former will dominantly contribute to the total loss at low

TABLE II D.c. magnetic properties of the uncoated ribbon and the ribbons coated with the oxides

Type of coated oxide	μ_i	μ_m	B_r/B_{10}	H_c (7.958×10^{-2} Am^{-1})
Uncoated	20 800	44 800	0.40	67
MgO	9 400	66 400	0.74	80
BaO	12 200	14 800	0.20	83
Al_2O_3	27 700	38 800	0.34	51
SiO_2	18 900	50 500	0.57	89
$MgO–Al_2O_3$	10 300	77 700	0.71	90
$CaO–Al_2O_3$	23 300	29 700	0.34	85
$SrO–Al_2O_3$	10 000	12 400	0.16	69
$BaO–Al_2O_3$	8 600	11 300	0.17	80
$MgO–SiO_2$	15 400	49 000	0.50	69

frequencies but the latter will be dominant at high frequencies.

This brief discussion indicates that, in order to understand the results for μ_e and W_L, detailed information on the domain structure is required. In an effort to obtain this information d.c. magnetic properties were measured and the results are summarized in Table II. The hysteresis results are plotted in Fig. 4(a–e) for some typical cases, namely for the uncoated ribbon and the ribbons coated with MgO, $MgO–Al_2O_3$, BaO, $SrO–Al_2O_3$, respectively. The values of coercivity H_c listed in Table II were obtained by applying a maximum field of 79.58 Am^{-1}. A very large difference in the d.c. magnetic properties is observed, which is vividly reflected in the shapes of the hysteresis graphs. The hysteresis loop for the ribbons coated with MgO and $MgO–Al_2O_3$ is square-shaped (more squared than the uncoated ribbon) with a large value of B_r/B_{10} (B_r is the remanent flux density and B_{10} is the flux density at the magnetic field of 795.8 Am^{-1}) and the maximum permeability, μ_m, but a small value of the initial permeability, μ_i. The squared-shape (and hence large B_r/B_{10}) may be related to the fact that more domains are aligned in the length direction [19]. The low value of μ_i may be related to a low domain density, since magnetization by domain wall movement and domain wall bending is expected to be small when the domain density is small. From this, the ribbons coated with these single and double metal oxides are considered to have a small number of domains and a large proportion of these domains are aligned in the length direction. The shape of the hysteresis graphs for the ribbons coated with BaO, $SrO–Al_2O_3$ and $BaO–Al_2O_3$ are significantly inclined with a small value of B_r/B_{10}. The values of μ_m and μ_i are small as is expected. It is important to note that the difference in the values between μ_m and μ_i is small for these ribbons. These d.c. results may indicate that more domains are aligned in the transverse direction. Detailed information on the domain density cannot be drawn from the present d.c. results. However, from geometrical considerations the domains of these ribbons are considered to be more refined than for the ribbons with squared hysteresis loops, since a large domain width results in a very large magnetostatic energy when the domains are aligned in the transverse direction. The shape of the hysteresis loop for the ribbon coated with SiO_2 is squared and with Al_2O_3 it is slightly inclined, whilst no substantial change in the d.c. properties was observed for the MgO coating. In most cases, the value of H_c was appreciably increased by the coating with the notable exception of the Al_2O_3 coating.

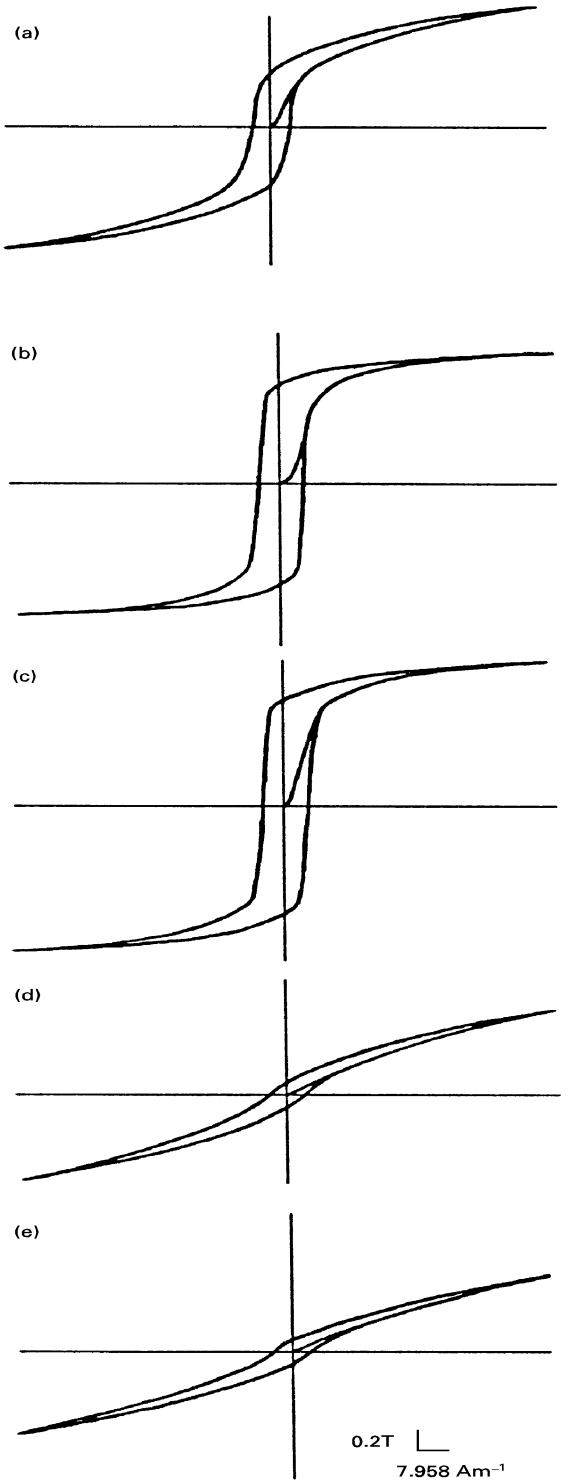

Figure 4 D.c. hysteresis loops for (a) the uncoated ribbon and the ribbons coated with (b) MgO, (c) $MgO–Al_2O_3$, (d) BaO, (e) $SrO–Al_2O_3$.

The results for the d.c. properties and information drawn from these d.c. results may offer some explanation for the μ_e and W_L results shown in Figs 1 and 2. The μ_e results can be explained by using the correlation between μ_e and B_r/B_{10} investigated by Lim *et al.*

for amorphous alloys [10, 18]. The results indicate that a material with a high B_r/B_{10} has a high value of μ_e at low frequencies and that μ_e steeply decreases with the frequency resulting in a low value of μ_e at high frequencies. A material with a low B_r/B_{10}, on the other hand, has a low value of μ_e at low frequencies and this small value of μ_e is maintained up to very high frequencies. In fact, in most cases, the current μ_e results are satisfactorily explained by the correlation behaviour although some minor disagreements are seen in the cases of ribbons coated with Al_2O_3 and SiO_2, where some other factor that affects μ_e must be introduced. For example, the slightly improved permeability of the Al_2O_3 coated ribbon compared to the uncoated ribbon may be related to the low value of H_c. The high values of W_L observed for the ribbons coated with MgO, SiO_2 and MgO–Al_2O_3 are thought to result from the low domain density which results in a large anomalous loss. Similarly, the low loss values observed for the ribbons coated with BaO and BaO–Al_2O_3 may result from a refined domain structure. The very low losses for the ribbon coated with Al_2O_3 does not appear to be explained in terms of the domain structure; again, this may be related to the very low value of H_c which reduces the hysteresis loss component. As previously mentioned the hysteresis loss is one of the two important components that contribute to the total loss.

It would be of interest to consider the reasons behind the large change in the magnetic properties caused by the surface coating. The main reason is thought to result from the magnetoelastic effect which is caused by coupling the magnetostriction to the stress induced by the coating. Since the present Fe-based amorphous alloy has a positive magnetostriction (whose value is relatively high at 20×10^{-6}), a tensile stress in the length direction causes domains to align in the length direction, thus resulting in a square-shaped hysteresis loop with a high value of B_r/B_{10} [20]. Similarly, a compressive stress leads to an inclined hysteresis graph with a low value of B_r/B_{10} [20]. It is therefore thought that the MgO and MgO–Al_2O_3 coatings induce a tensile stress while those of BaO, SrO–Al_2O_3 and BaO–Al_2O_3 induce a compressive stress. The other oxides do not seem to induce any appreciable amounts of stress.

The various induced stress types that are obtained depending on the type of the coating oxide used may be of practical importance. The coatings play a similar role to field and stress annealing. Considering that the formation of induced anisotropy in the transverse direction by field annealing is known to be difficult and the induced anisotropy energy is small in the case of Fe-based amorphous alloys [21], the inclination of the hysteresis loop by the coating is particularly important. In applications such as choke cores, constant permeability over a wide applied field is an important property, which may be achieved by inducing anisotropies in the transverse direction. A rough estimate shows that the energy of induced anisotropy achieved by the present coating is of the order of 100 $J\,m^{-3}$. A field annealing of a coated ribbon in the transverse direction is expected to further increase the induced anisotropy energy. Work in this direction is in progress and will be published in due course.

4 Conclusions

The metal oxides MgO, BaO, Al_2O_3, SiO_2, MgO–Al_2O_3, CaO–Al_2O_3, SrO–Al_2O_3, BaO–Al_2O_3, and MgO–SiO_2 have been coated onto ribbons of the Fe-based amorphous alloy Metglas 2605S3A using a sol–gel process. The effects on the magnetic properties of the alloy of the surface coating have been investigated. A more square-shaped hysteresis loop was observed for ribbons coated with MgO and MgO–Al_2O_3 but a more inclined loop was observed for the ribbons coated with BaO, SrO–Al_2O_3 and BaO–Al_2O_3 than for the uncoated ribbon. The frequency dependence of the effective permeability is also significantly affected by the oxide coating. A ribbon coated with MgO–Al_2O_3, for example, exhibits substantially higher values of the permeability than the uncoated ribbon over the whole measured frequency range, whilst, in the case of ribbons coated with BaO, BaO–Al_2O_3 and SrO–Al_2O_3, the permeability is low at low frequencies but it remains relatively constant up to very high frequencies. The core loss is also affected by the coating, although the difference is not so significant dependant on the type of the coated oxide. These results may be explained by a stress induced by the coating and the modification of the domain structure via elastic and/or magnetoelastic interactions. It is considered from the magnetoelastic interactions that the MgO and MgO–Al_2O_3 coatings induce tensile stresses whilst those of BaO, SrO–Al_2O_3 and BaO–Al_2O_3 induce compressive stresses.

References

1. D. M. NATHASINGH, C. H. SMITH and A. DATTA, *IEEE Trans. Magn.* **MAG-20** (1984) 1332.
2. S. TAGUCHI, T. YAMAMOTO and A. SAKAKURA, *Ibid.* **MAG-10** (1974) 123.
3. D. R. THORNBURG and W. M. SWIFT, *Ibid.* **MAG-15** (1979) 1592.
4. Y. INOKUTI, K. SUZUKI and Y. KOBAYASHI, *J. Jpn. Inst. Met.* **59** (1995) 213.
5. Y. INOKUTI, *Ibid.* **59** (1995) 347.
6. S. H. LIM, Y. S. CHOI, Y. J. BAE, H. K. CHAE, T. H. NOH and I. K. KANG, *IEEE Trans. Magn.* **MAG-31** (1995) 3898.
7. D. C. BRADLEY, R. C. MCHROTRA and D. P. GAUR in "Metal alkoxides", (Academic, London, 1978) Ch. 2 and Ch. 5.
8. M. MITERA, H. FUJIMORI and T. MASUMOTO, in "Rapidly quenched metals", Vol. II, edited by T. Masumoto and K. Suzuki (The Japan Institute of Metals, Sendai, Japan, 1982) p. 1035.
9. H. FUJIMORI, H. MORITA, M. YAMAMOTO and J. ZHANG, *IEEE Trans. Magn.* **MAG-22** (1986) 1101.
10. S. H. LIM, Y. S. CHOI, T. H. NOH and I. K. KANG, *J. Appl. Phys.* **75** (1994) 6937.
11. M. KERSTEN, *Physik. Z.* **39** (1938) 860.
12. S. CHIKAZUMI in "Physics of magnetism", (J. Wiley, New York, 1964) Ch. 13.
13. D. JILES, in "Introduction to magnetism and magnetic materials", (Chapman and Hall, London, 1991) Ch. 7.
14. R. H. PRY and C. P. BEAN, *J. Appl. Phys.* **29** (1958) 532.

15. H. PFUTZNER, P. SCHONHUBER, B. ERBIL, G. HARASKO and T. KLINGER, *IEEE Trans. Magn.* **MAG-27** (1991) 3426.
16. R. F. KRAUSE and F. E. WERNER, *Ibid.* **MAG-17** (1981) 2686.
17. V. R. V. RAMANAN, *J. Mater. Engng.* **13** (1991) 119.
18. S. H. LIM, Y. S. CHOI, T. H. NOH and I. K. KANG, (unpublished results).
19. S. CHIKAZUMI, in "Physics of magnetism", (J. Wiley, New York, 1964) Ch. 12.
20. B. D. CULLITY, in "Introduction to magnetic materials", (Addison-Wesley, Reading MA, 1972) Ch. 12.
21. A. HERNANDO and M. VAZQUEZ, in "Rapidly solidified alloys", edited by H. H. Lieberman (Marcel Dekker, New York 1993) Ch. 17.

Received 7 March
and accepted 31 July 1996